

# Theoretical Estimation of Electromigration in Metallic Carbon Nanotubes Considering Self-Heating Effect

Rekha Verma, *Student Member, IEEE*, Sitangshu Bhattacharya, and Santanu Mahapatra, *Senior Member, IEEE*

**Abstract**—In this paper, we estimate the solution of the electromigration diffusion equation (EMDE) in isotopically pure and impure metallic single-walled carbon nanotubes (CNTs) (SWCNTs) by considering self-heating. The EMDE for SWCNT has been solved not only by invoking the dependence of the electromigration flux on the usual applied static electric field across its two ends but also by considering a temperature-dependent thermal conductivity ( $\kappa$ ) which results in a variable temperature distribution ( $T$ ) along its length due to self-heating. By changing its length and isotopic impurity, we demonstrate that there occurs a significant deviation in the SWCNT electromigration performance. However, if  $\kappa$  is assumed to be temperature independent, the solution may lead to serious errors in performance estimation. We further exhibit a tradeoff between length and impurity effect on the performance toward electromigration. It is suggested that, to reduce the vacancy concentration in longer interconnects of few micrometers, one should opt for an isotopically impure SWCNT at the cost of lower  $\kappa$ , whereas for comparatively short interconnects, pure SWCNT should be used. This tradeoff presented here can be treated as a way for obtaining a fairly well estimation of the vacancy concentration and mean time to failure in the bundles of CNT-based interconnects.

**Index Terms**—Electromigration, metallic carbon nanotubes (CNTs), self-heating, thermal conductivity.

## I. INTRODUCTION

ELECTROMIGRATION in aggressively scaled interconnects is one of the key factors in understanding the mean time to failure (MTTF) of modern integrated circuits (ICs). As the downscaling of ICs continues, current densities inside the chip are being pushed to their respective limits. This initiates the onset of Joule heating along the interconnect length which degrades its reliability and results in the consequent failure of the chip. Conventional interconnect materials like Cu and Al have limited current-carrying capacity of about  $10^6 \text{ A} \cdot \text{cm}^{-2}$  and thermal conductivities of 401 and  $237 \text{ W} \cdot \text{m}^{-1} \cdot \text{K}^{-1}$  at room temperature, respectively [1]. To surpass the existing performance level of Cu/Al, carbon nanomaterials have been

found to withstand and possess a very high reportedly breakdown current density and thermal conductivity which are on the order of  $10^8$ – $10^9 \text{ A} \cdot \text{cm}^{-2}$  [1]–[3] and  $600$ – $7000 \text{ W} \cdot \text{m}^{-1} \cdot \text{K}^{-1}$  [4], respectively, thus making them good candidates for electrothermal materials. However, their potential to resist electromigration is one of the bottleneck issues of IC reliabilities and is currently grasping attention [2]. Recently, there have been a few experimental studies that predicted the self-heating in metallic single-walled carbon nanotubes (CNTs) (SWCNTs) [3], [5], but the theoretical approach in justifying this was based on the assumption of a constant thermal conductivity beyond room temperature [6], which later evolved in an empirical dependence [3]. Lately, using different scattering phenomena like isotope scattering, as also established through a recent experiment [7] which essentially reflects the presence of  $^{13}\text{C}$  atom isotope on pure  $^{12}\text{C}$  atom in carbon nanomaterials, thus making the system impure, the three-phonon Umklapp and boundary scatterings led to the explanation of the extreme nonlinear variation of  $\kappa$  [8], which was found to be in good agreement with the available experimental data [3], [5]. This variation results in an involved mathematical formulation of the solution of self-heating equation [3] for both isotopically pure and impure cases, which should be taken into account for the temperature distribution along its length [9]. It is this temperature distribution which should be included in the vacancy flux current density  $J_v$  at extreme electromigration test current levels for the determination of the vacancy concentration and the MTTF [10], [11].

The novelty of the solution of electromigration diffusion equation (EMDE) in this paper lies in order to incorporate the self-heating along a finite-length metallic SWCNT and to demonstrate its effect on the electromigration performance. Since the difficulties in the fabrication of horizontally aligned local, intermediate, and global interconnects using SWCNT bundles are one of the bottleneck issues in recent interconnect technology, ease in incorporation of their bundles as vias demands that an efficient solution of the EMDE in a single metallic SWCNT should be the first step in the investigation of an accurate electromigration model of the overall bundles. Keeping this in focus, the objective of this paper is to address the solution of the EMDE for the investigation of distribution of the vacancy concentration and lifetime in a single metallic SWCNT of finite length at a perfectly blocking diffusion barrier under self-heating condition. The methodologies as presented here can then be put forward for obtaining a fairly well

Manuscript received February 21, 2012; revised May 10, 2012; accepted May 28, 2012. Date of publication July 10, 2012; date of current version August 17, 2012. The review of this paper was arranged by R. Venkatasubramanian.

The authors are with the Nanoscale Device Research Laboratory, Department of Electronic Systems Engineering (formerly CEDT), Indian Institute of Science, Bangalore 560 012, India (e-mail: rekha.verma26@gmail.com; isbsin@yahoo.co.in; santanu@cedt.iisc.ernet.in).

Digital Object Identifier 10.1109/TED.2012.2202909

estimation of the electromigration effects on the dielectrically surrounded CNT bundles.

## II. SIMULATION METHODOLOGY AND DISCUSSIONS

The investigation on electromigration dates back to 1969 in explaining the failure of Al-based materials by a number of test experiments done by Black [12] under extreme high currents and temperature, beyond normal values. Based on his experimental results, Black formulated the MTTF for the estimation of the lifetime of a device which is widely adapted by the IC process technology and is generally written as [13]

$$MTTF = \frac{A}{j^n} \exp\left(\frac{E_A}{k_B T}\right) \quad (1)$$

in which  $A$  involves the interconnect cross-sectional dimensions and other characteristic constants and  $j$ ,  $E_A$ ,  $k_B$ , and  $T$  are the current density, activation energy of the interconnect material, Boltzmann's constant, and temperature along the length of the interconnect, respectively. The basic approach to derive this equation was based on the estimation of the rate of concentration of the vacancies ( $C_v$ ) along the length of the Al interconnect. The exponent  $n$  is a topic of debate which may have a value in the range from as low as 2 to as high as 16 for the description of self-heating along the length [14]. Theoretically, Shatzkes and Lloyd [11] used the effect of Fickian diffusion and mass transport due to the driving force to explain that this exponent  $n$  should take the value of two. Assuming a linear relationship between the vacancy and atomic diffusivity, Clement [14] obtained the relation of MTTF as

$$MTTF = \frac{A'}{j^2} \exp\left(\frac{E_A}{k_B T}\right) \quad (2)$$

where  $A' = A = \psi_f [D_0 (C/C_v) (q^* \rho / k_B T)^2]^{-1}$ ,  $D_a = D_0 \exp(-E_A/k_B T)$ , and  $D_0$  are the average atomic and self-diffusivities,  $C$  is the lattice site concentration assumed to be nearly equal to atomic vacancy ( $C_a$ ),  $q^* = |Z^*|e$  is the effective charge with  $e$  as electron charge,  $|Z^*|$  is the measure of ion-electron interaction generally in the range of 1–2 [14],  $\rho$  is the longitudinal electrical resistivity of the interconnect, and  $\psi_f$  is the critical vacancy concentration before the steady state is reached.

The electromigration diffusion continuity equation can be written following the mass conservation law as [15]

$$\vec{\nabla} \cdot \vec{J} + \frac{\partial C}{\partial t} = 0. \quad (3)$$

In general, the quantity  $\vec{J}$  is the vector sum of all the current densities due to driving forces, primarily of which are the electron-wind force arising due to the applied longitudinal static electric field

$$\vec{J}_{EW} = \frac{C}{k_B T} |Z^*| e \rho \vec{j} D_0 \exp\left(\frac{-E_A}{k_B T}\right) \quad (4)$$

the Fickian diffusion arising due to the concentration gradient force

$$\vec{J}_C = -D_0 \exp\left(\frac{-E_A}{k_B T}\right) \vec{\nabla} C \quad (5)$$

the stress gradient force

$$\vec{J}_S = \frac{C}{k_B T} V_0 D_0 \exp\left(\frac{-E_A}{k_B T}\right) \vec{\nabla} \sigma \quad (6)$$

and the thermal gradient force

$$\vec{J}_T = -\frac{C}{k_B T} Q^* D_0 \exp\left(\frac{-E_A}{k_B T}\right) \left(\frac{\vec{\nabla} T}{T}\right) \quad (7)$$

in which  $V_0$  is the volume per atom,  $\sigma$  is the hydrostatic stress, and  $Q^*$  is the coefficient of heat transfer.

In the case of Cu/Al, the strength of the stress and the thermal gradient forces as compared with that of the electron-wind forces is significantly higher [13], [16], and thus, one has to solve (3) using all the gradient forces defined earlier. However, as metallic SWCNT has the ability to withstand comparatively much higher currents, using (4), (6), and (7), we find that the strength of the stress and the thermal gradient forces turns out to be on the order of  $10^{-1}$ – $10^{-3}$  and can be treated as insignificant. Using this approximation, (3) can be written for a 1-D directed current density as

$$\frac{\partial C}{\partial t} - D_a \frac{\partial}{\partial x} \left( \frac{\partial C}{\partial x} - \frac{Z^* e E}{k_B T} C \right) = 0 \quad (8)$$

where  $E$  is the applied electric field. This equation has been derived under the further assumption of a constant average mass transport atomic diffusion coefficient [17]. In the case of metallic SWCNT under the condition of self-heating effect, there occurs a significant temperature distribution along the length at very high current and very high impurity. This results in a nonlinear distribution of the temperature and thus cannot be treated as constant anymore. However, for a simplified analysis of the solution of EMDE, we assume the atomic diffusivity to be a slowly varying function of  $T$  over the length owing to the higher atomic inertia.

Using these assumptions, we proceed for the solution of EMDE under two cases.

### A. EMDE for an Isotopically Pure SWCNT

The rise in temperature along the length of a pure metallic SWCNT due to the result of self-heating when a current is passed through it, whose two ends are fixed at lower and higher temperatures ( $T_l$  and  $T_h$ ), can be written following [8] and [9] as

$$T(x) = T_l + \frac{E_1 \kappa_l b}{a} (\theta(x) - T_l) \quad (9)$$

where  $-L/2 < x < L/2$ ,  $L$  is the tube length along the  $x$ -direction, and  $\kappa_l$  is the thermal conductivity of the SWCNT

at lower temperature end whose expression at any temperature is [9]

$$\kappa(T) = \frac{1}{3E_1} \left( \frac{k_B}{2\pi^2 v_g} \right) \left( \frac{k_B \Theta_D}{\hbar} \right)^3 \left( \frac{v_g}{E_1 L} + T^2 \right)^{-1} \quad (10)$$

in which  $v_g = 10^4 \text{ m} \cdot \text{s}^{-1}$  is the phonon group velocity;  $\Theta_D = 1000 \text{ K}$  is the Debye temperature;  $\hbar = h/2\pi$  with  $h$  as the Planck's constant;  $E_1 = (32/27)\gamma^4 (k_B/Mv_g^2)\omega_B$  with  $\gamma = 1.24$ ,  $\omega_B = 28 \text{ GHz}$ , and  $M$  as the Gruneisen parameter, the phonon branch frequency at the zone boundary, and the mass of the carbon atoms, respectively [8], [9], [18]–[20];  $a = (1/3)(k_B/2\pi^2 v_g)(k_B \Theta_D/\hbar)^3$ ; and  $b = v_g/E_1 L$ . The function  $\theta_x$  can be written as [9]

$$\theta(x) = c_1 e^{\alpha_1 x} + c_2 e^{-\alpha_1 x} - \frac{\beta_1}{\alpha_1^2} \quad (11)$$

where

$$c_1 = \left[ (\theta_h + \theta_l + 2\beta_1/\alpha_1^2) \sinh\left(\frac{\alpha_1 L}{2}\right) + (\theta_h - \theta_l) \cosh\left(\frac{\alpha_1 L}{2}\right) \right] \times \left[ 4 \sinh\left(\frac{\alpha_1 L}{2}\right) \cosh\left(\frac{\alpha_1 L}{2}\right) \right]^{-1} \quad (12)$$

$$c_2 = \left[ (\theta_h + \theta_l + 2\beta_1/\alpha_1^2) \sinh\left(\frac{\alpha_1 L}{2}\right) - (\theta_h - \theta_l) \cosh\left(\frac{\alpha_1 L}{2}\right) \right] \times \left[ 4 \sinh\left(\frac{\alpha_1 L}{2}\right) \cosh\left(\frac{\alpha_1 L}{2}\right) \right]^{-1} \quad (13)$$

in which  $\theta_l = T_l$ ;  $\theta_h = T_l + (a(T_h - T_l)/E_1 b \kappa_l)$ ;  $\alpha_1^2 = (\alpha_2^2 E_1 b/a)$  where  $\alpha_2^2 = (g/A)$ ;  $\beta_1 = ((\beta/\kappa_l) - (\alpha_2^2 E_1 b T_l/a) + (\alpha_2^2 T_l/\kappa_l))$  where  $\beta = -(p + gT'/A)$  with  $T' = (1/2)(T_h + T_l)$ ,  $g$  as the net heat loss to the substrate per unit length, and  $p = j^2(\rho(T) - \rho_c)A$  wherein  $\rho(T)$  and  $\rho_c$  are the total electrical resistivities of the nanotube and contacts, respectively, and  $A = \pi d b_1$  is the cross-sectional area with  $d$  and  $b_1$  as the diameter and the tube wall thickness of the SWCNT, respectively. It should be noted that, in this case, we have taken the Gruneisen parameter to be 1.24 [8], [9], [18]. Furthermore, we took the CNT Debye temperature to be 1000 K, although there are few references, for example, Wang *et al.* [19], which consider  $\Theta_D = 30 \text{ K}$ . However, for the present purpose, we took the value from Hone *et al.* [20]. The value of 30 K, shown in this paper, is only the first subband energy (2.7 meV). Theoretically, the effective Debye energy is 103 meV while a fitted value from measurement exhibits 92 meV, which implies that the Debye temperature is around 1000 K. In addition to making the analyses simple and a closed one, we have assumed the usual identity of the Debye integrand in the higher temperature zone, i.e., the term  $x^2 e^x/(e^x - 1)^2$  approaches unity by taking the three-phonon Umklapp scattering rate [9], [21]. As far as (10) is concerned, the thermal conductivity exhibits a  $T^{-2}$  falling rate which is a well-established phenomenon through experiments, for example, Pop *et al.* [6]. The relative error which may appear using these assumptions by particularly bypassing the method of extensive numerical solution [22] for achieving a very high

accurately determined thermal conductivity, to our belief, will not throw significant error and will remain under the experimental error range.

The use of (9) and (11) in (8) results in a normalized EMDE as

$$\frac{\partial \nu}{\partial \zeta} - \frac{\partial}{\partial \xi} \left( \frac{\partial \nu}{\partial \xi} - \alpha(\xi) \nu \right) = 0 \quad (14)$$

where  $\alpha(\xi) = \alpha_B(\xi)L$  in which  $1/\alpha_B(\xi) = k_B T(\xi)/|Z^*|e\rho_j$  is the distance over which the steady-state concentration profile at any temperature  $T$  in a finite-length conductor is reduced to 36.7% of its maximum value and is defined as the Blech length [10], [17], [23] at that temperature and  $\xi = x/L$ ,  $\zeta = D_a t/L^2$ , and  $\nu = C/C_0$  are the normalized variables for the reduced length, time, and vacancy concentration, respectively, whereas  $C_0$  is the equilibrium vacancy concentration.

Thus, it can be seen that the solution of (14) in this general form is an extremely involved mathematical task and cannot be obtained over the length. However, if the Blech length is independent of the temperature variation, there exists a closed-form solution for both finite- and infinite-length conductors. Under the general boundary conditions considering a temperature-dependent Blech length, one finds [10]

$$J\left(\frac{L}{2}, t\right) = D_a \left\{ \frac{\partial C\left(\frac{L}{2}, t\right)}{\partial x} - \alpha C\left(\frac{L}{2}, t\right) \right\} = 0 \quad (15)$$

$$C(-\infty, t) = C_0 \quad (16)$$

$$J\left(-\frac{L}{2}, t\right) = 0 \quad (17)$$

$$C\left(-\frac{L}{2}, t\right) = C_0. \quad (18)$$

The solution of (14) including all the aforementioned boundary conditions has been analytically shown for Cu/Al interconnects where the Blech length is dependent on temperature variation [10], [11], [14], [23]. However, of the aforementioned listed four boundary conditions, it was analyzed that, using (18), saturation was achieved at a much higher vacancy concentration which is in good agreement with the experimental data exhibiting a strong passivation layer [10]. We thus use (18) to solve (14) numerically to estimate the evolution of vacancy distribution for different lengths and different current levels both as functions of normalized time and length, respectively. The present solution of (14) thus focuses on the distribution of vacancy concentration over the length of the SWCNT by invoking the rudimentary temperature-dependent thermal conductivity model. It is now well known that the  $\kappa$  of SWCNT is a strong function of temperature beyond the room temperature [3], [4], [6]. Solving the Joule-heating equation [9] using this  $\kappa$  establishes the temperature distribution over the SWCNT length. This temperature profile widely differs from the temperature profiles of Cu/Al metal lines under identical conditions since  $\kappa$  of Cu/Al is almost temperature independent in the region 300 K and above. This is the cause why the Blech length in SWCNT widely differs from that of Cu/Al. We also have extended this study for an isotopically impure SWCNT as we

shall see in Section II-B, where  $\kappa$  changes strongly both with the temperature and the addition of isotope impurity.

Figs. 1 and 2 show the ratio of the vacancy concentration at the blocking barrier to its equilibrium value  $[C((L/2), t)/C_0]$  as a function of normalized time, where we choose four current levels for a 2-nm-diameter SWCNT, viz., 0.1, 1, 3, and 5  $\mu\text{A}$ , corresponding to current densities of 0.468, 4.68, 14.044, and  $23.408 \times 10^{11} \text{ A} \cdot \text{m}^{-2}$ , respectively, which are quite higher than those of the existing ITRS-based 22-nm technology node for Cu/Al interconnects [1] to estimate the electromigration performance of metallic SWCNT. We choose the temperatures at the two ends to be 300 K and 450 K which physically exhibit the temperature levels at the substrate and heat sink point. It should particularly be noted that the choice of the temperature levels and the current levels is based strictly on the respective design applications of the IC [24]–[26]. Using these values and  $\rho = 10^{-7} \Omega \cdot \text{m}$  for metallic SWCNT, the said figures exhibit the saturation levels of the vacancy concentrations for 0.5- and 1- $\mu\text{m}$ -long tubes. In the same figures, for comparison, we have also plotted all the corresponding cases by taking a constant thermal conductivity. It appears from Fig. 1 that, for a comparatively shorter length, the vacancy concentration saturates, with much less magnitude, nearly at the same value for all the current levels thus resisting electromigration, a remarkable feature which does not prevail for Cu/Al interconnects, not even also under identical conditions. The assumption of a constant thermal conductivity leads to an erroneous determination of the vacancy concentration levels as also exhibited in the same figure. Furthermore, all the curves for all the respective currents, both assuming a temperature-independent  $\kappa$  and temperature-dependent  $\kappa$ , tend to coincide below the saturation. The nature of fall being a parabolic shape exhibits that the MTF follows a  $j^{-2}$  dependence. The solution of the differential (14) for the boundary condition (16) is the main reason why the MTF follows a  $j^{-2}$  law. This boundary condition means a semi-infinite 1-D conductor situation. This is a well-known mathematical solution and has been described elsewhere [11]. Fig. 2 shows the length effect of the normalized vacancy when compared with Fig. 1. It appears that, with the increasing length, the lower current values do not tend to modify the magnitude of the vacancy concentration significantly; however, for larger currents, the vacancy concentration rises sharply and reaches about 100 times of the former. This sharp rise is due to the deviation of the Blech length from the length of the tube, which increases the vacancies at the blocking boundary. We thus see that a high current through a long tube results in the formation of high vacancy concentration in the presence of self-heating. We also note from these figures that, with increasing current, irrespective of the lengths, it takes longer time for the vacancy concentration to reach its saturation value. This is due to the reason that the electron-wind current density tends to dominate the Fickian diffusion current density, and thus, late saturation is expected. This can be justified in the sense that the two current densities in this paper incorporate the electron-wind force and the Fickian diffusion current. The electron-wind force contains the drift part and is thus proportional to the applied static longitudinal electric field. As the field increases, the drift part dominates over the diffusion part and thus mainly contributes

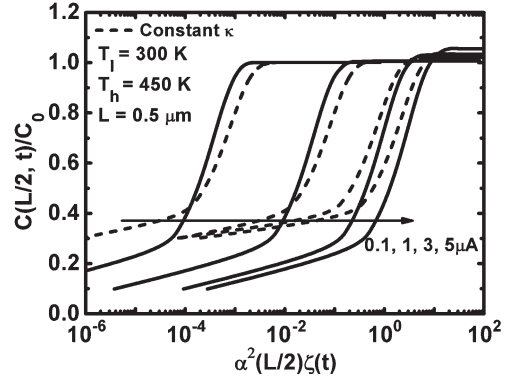


Fig. 1. Normalized vacancy concentration distribution at the blocking barrier for an isotopically pure SWCNT as a function of normalized time using (19) and the boundary condition (18) in (14) considering self-heating in a 0.5- $\mu\text{m}$ -long tube at different current levels. The dashed lines exhibit the corresponding cases for constant thermal conductivity, while the solid lines represent a temperature-dependent  $\kappa$ .

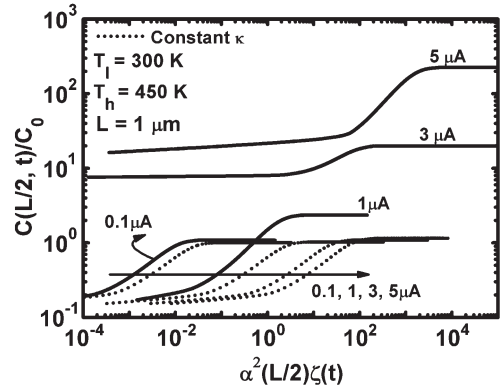


Fig. 2. Normalized vacancy concentration distribution at the blocking barrier for an isotopically pure SWCNT as a function of normalized time for all the cases in Fig. 1 for a 1- $\mu\text{m}$ -long tube.

to the variation of the vacancy concentration over the SWCNT length in time.

### B. EMDE for an Isotopically Impure SWCNT

The temperature distribution along the length of an isotopically impure SWCNT due to the presence of mass difference (MD) and Umklapp and boundary scatterings can be written as [9]

$$T(x) = T_l + \frac{\kappa_l T_l^2 E_1}{\lambda} (\theta(x) - T_l) \quad (19)$$

in which

$$\theta(x) = c_3 e^{\alpha_3 x} + c_4 e^{-\alpha_3 x} - \frac{\beta_2}{\alpha_3^2} \quad (20)$$

where

$$c_3 = \left[ (\theta_h + \theta_l + 2\beta_2/\alpha_3^2) \sinh\left(\frac{\alpha_3 L}{2}\right) + (\theta_h - \theta_l) \cosh\left(\frac{\alpha_3 L}{2}\right) \right] \times \left[ 4 \sinh\left(\frac{\alpha_3 L}{2}\right) \cosh\left(\frac{\alpha_3 L}{2}\right) \right]^{-1} \quad (21)$$

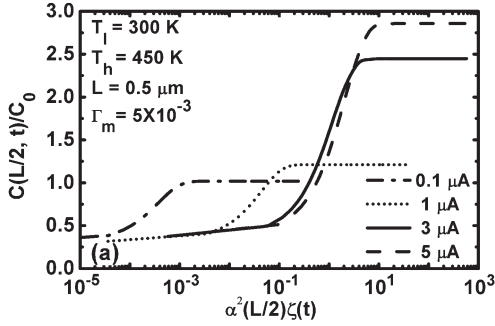


Fig. 3. Normalized vacancy concentration distribution at the blocking barrier in an isotopically impure SWCNT as a function of normalized time using (19) and the boundary condition (18) in (14) considering self-heating using (23) for 0.5- $\mu\text{m}$ -long tube.

$$c_4 = \left[ (\theta_h + \theta_l + 2\beta_2/\alpha_3^2) \sinh\left(\frac{\alpha_3 L}{2}\right) - (\theta_h - \theta_l) \cosh\left(\frac{\alpha_3 L}{2}\right) \right] \times \left[ 4 \sinh\left(\frac{\alpha_3 L}{2}\right) \cosh\left(\frac{\alpha_3 L}{2}\right) \right]^{-1} \quad (22)$$

$\alpha_3^2 = \alpha_2^2 E_1 T_l^2 / \lambda$ ;  $\beta_2 = (\beta/\kappa_l) + (\alpha_2^2 T_l / \kappa_l) - (\alpha_2^2 E_1 T_l^3 / \lambda)$ , where  $\lambda = (k_B / 2\pi^2 v_g) (4\pi v_g^4 / LV_0 \Gamma_m)^{3/4}$  with  $\Gamma_m$  as the dimensionless strength of the MD scattering and  $\kappa_l$  in this case is the impure SWCNT thermal conductivity whose temperature-dependent form for the present impure case is [9]

$$\kappa(T) = \lambda \left( E_1 T^2 + \frac{v_g}{L} \right)^{-1}. \quad (23)$$

Fig. 3 shows the numerical estimation of the vacancy concentration ratio at the blocking boundary in an impure SWCNT considering (23) and using (19) and (18) in (14).

It appears from Fig. 3 that, with the increase in the isotope impurity to a value  $\Gamma_m = 5 \times 10^{-3}$ , the magnitude of the vacancy concentration increases as compared to the corresponding cases in Fig. 1 at pure condition. It should be noted that the quantity  $\Gamma_m$  describes the amount of isotopic impurity in a pure material responsible for point defect or MD phonon scattering. The value of  $\Gamma_m$  on the order of  $10^{-3}$  is indeed quite a large value for nanowires arresting a very high reduction in phonon-assisted thermal conductivity [7], [27]. Since electromigration testing is generally done at the extreme values, we thus have chosen the very high value of  $\Gamma_m = 5 \times 10^{-3}$ . Generally,  $10^{-7}$  stands as nearly pure sample and suppresses the MD scattering thereby increasing the thermal conductivity. However, as  $\Gamma_m$  goes on increasing in the  $^{13}\text{C}$  isotopes as impurity on  $^{12}\text{C}$  SWCNT, the thermal conductivity falls which raises the temperature along with the Joule heating through the CNT length. This is the main reason why the magnitude of the vacancy concentration increases. Also, in the same curve, we see that increasing the current beyond a certain level sharply increases the saturation level of the vacancy concentration exhibiting the electron-wind force dominance over Fickian diffusion force; however, the onset of saturation in both cases in Figs. 1 and 3 is almost the same. Interestingly, from Fig. 4 for longer tube, we see that the saturation magnitude of the vacancy concentration in impure SWCNT falls 100 times below the corresponding case of pure SWCNT at high currents

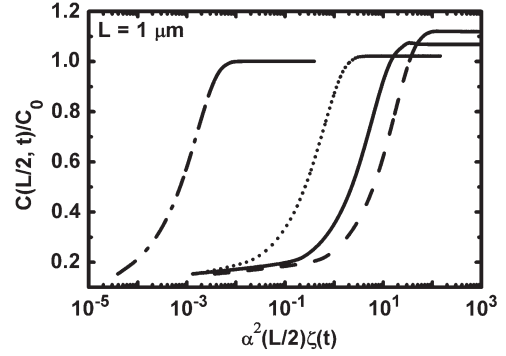


Fig. 4. Normalized vacancy concentration distribution at the blocking barrier in an isotopically impure SWCNT as a function of normalized time for all cases in Fig. 3 for 1- $\mu\text{m}$ -long tube.

exhibiting the physical fact that the Blech length approaches the tube length. This modulation of the Blech length roots in the variation of the thermal conductivity to a desired value of operation by adding isotopic impurities. With the increase in impurity, the thermal conductivity decreases which increases the temperature distribution along the length to a much higher value, thus increasing the Blech length. As the Blech length approaches the tube length, the vacancy concentration at the blocking boundary tends to 36.7% of its initial equilibrium value. However, in the case of comparatively shorter length for pure SWCNT, we see that the saturation level of the vacancy concentration at the blocking boundary is lower than that of the corresponding impure case. This is because of the fact that metallic pure SWCNT results in a higher thermal conductivity which brings down the temperature distribution along its length which further reduces the Blech length. Thus, for a shorter length, the saturation magnitude of the vacancy concentration reduces than that of the corresponding impure case.

The distribution of normalized vacancy concentration over the SWCNT length is shown in Figs. 5 and 6 for both pure and impure cases, respectively. We see in the case of pure SWCNT that, as the current increases, the vacancy ratio at the blocking boundary increases with length. However, in the case of impure SWCNT, the vacancy concentration decreases with the increase in both current and length. It thus appears from comparing Figs. 5 and 6 that the sign of the slope of the vacancy ratio changes sharply when one increases the impurity. By considering the activation energy of SWCNT to be 1.265 eV [28], using (2), we estimate the lifetime of the SWCNT interconnects as a function of current density at a temperature of 450 K in Fig. 7. Since the proper values of the atomic diffusivity and the lattice concentration have not been reported yet, we have plotted the lifetime with the inclusion of different values of the inverse diffusivity parameter  $\gamma = \psi_f [D_0 (C/C_v)^2]^{-1}$  ranging from  $10^4$  to  $10^8 \text{ s} \cdot \text{m}^{-2}$ . This demands a deeper physical look for understanding the effect of self-heating in SWCNT on the lifetime. At this point, it should be noted that the MTTF, in general, depends on both the current density and the temperature. However, at very high currents, i.e., in the case of self-heating, the current density and temperature are inherently coupled through the two carrier transport parameters, viz., the electrical resistance and the

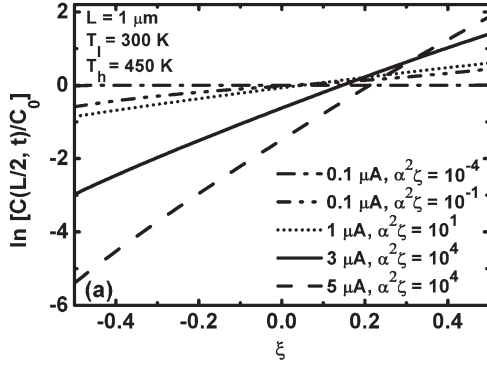


Fig. 5. Normalized vacancy concentration distribution at the blocking barrier as a function of normalized length for an isotopically pure SWCNT in which  $10^{-4}$  and  $10^{-1}$  correspond to normalized time values before and at the saturation level, whereas  $10^1$  and  $10^4$  correspond to the normalized time values beyond saturation level.

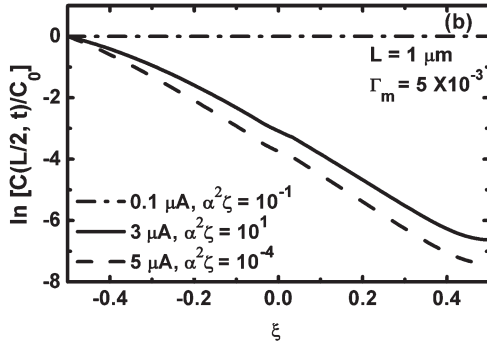


Fig. 6. Normalized vacancy concentration distribution at the blocking barrier as a function of normalized length for an isotopically impure SWCNT in which  $10^{-4}$ ,  $10^{-1}$ , and  $10^1$  correspond to normalized time values before the saturation level, at the saturation level, and beyond the saturation level, respectively.

thermal conductivity. In the case of SWCNT, the ability of changing  $\kappa$  results in a nonlinear temperature distribution over its length where the difference of the temperature between the two ends is significantly high. This variation in the temperature causes a temperature-dependent resistance which again controls the magnitude of  $j$ . Thus, from the MTTF equation, we expect a dependent relation between  $j$  and  $T$ . Moreover, the functions  $\psi$  and  $C/C_v$  in this present case depend not only on the amount of heating current but also on the purity of the SWCNT. From Figs. 1–6, it can be compared that the effect of increasing the impurity in longer SWCNT aids in reducing the vacancy concentration thus resisting the electron-wind and Fickian diffusion forces. This provides an expected longer lifetime for longer impure SWCNTs and also follows for comparatively short and pure SWCNTs.

All the curves in Fig. 7 have been presented by neglecting the coupled relations between  $j$ ,  $T$ ,  $\psi$ , and  $C/C_v$ . However, from Fig. 7, one can easily estimate the lifetime in the case of impure SWCNT. The inclusion of these effects would certainly increase the accuracy of the results, although our suggestion for the estimation of lifetime would not change in the presence of the aforementioned effects. Our model is in the range of few tenths of micrometers to few micrometers over which the resistance is almost independent of temperature [3]. In Fig. 7, we

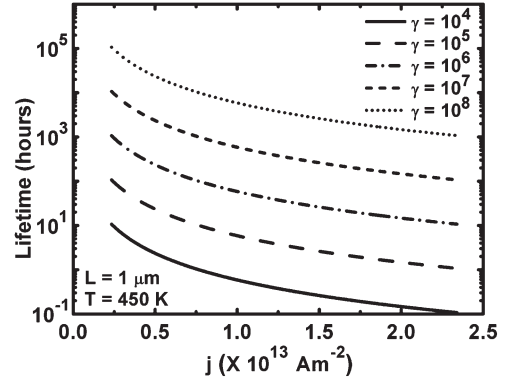


Fig. 7. Lifetime of metallic SWCNT as a function of current density.

have neglected this issue. The effect of impurity on the MTTF is also neglected in Fig. 7 which, to our understanding, should be considered. This is so because an increase in the impurity increases the temperature variation which again affects the resistance and consequently the  $j$ . The reason for this omission is due to the absence of a proper analytical expression that captures this complete electrothermal picture, which, however, at this stage, is beyond the scope of this paper.

The work presented here signifies the estimation of the interconnect lifetime and the vacancy concentration values for interconnect length in the range of 500 nm–2  $\mu\text{m}$ . This is so because, below 500-nm tube length, the thermal conductivity exhibits ballistic nature due to the lattice phonon quantization [19], [29]. However, the electrical resistance switches to diffusive mode from nearly above 2  $\mu\text{m}$  beyond room temperature [3]. Accordingly, this stands as the length zone of validation of the solution of Joule-heating equation in this paper in the temperature zone of 300 K–450 K where both the electrical and phonon resistances are diffusive. We have not considered the length zone above 2  $\mu\text{m}$  where the electrical resistance becomes a function of the temperature [3] which terribly complicates the self-heating equation. At this stage, considering these effects in the determination of electromigration performance in the bundles as vias is not fully understood due to the unavailability of experimental data for proper theoretical justifications. The methodologies as presented in this paper can be used as the first step to estimate the electromigration performance of the bundles of metallic SWCNT surrounded by the dielectric by considering the effect of the electrothermal crosstalks.

### III. CONCLUSION

In this paper, we have presented an estimation of the effect of electromigration forces on the performance of metallic SWCNT in the presence of self-heating. It has been suggested that, to increase the immunity toward the electromigration forces for longer interconnects, one should opt for an isotopically impure SWCNT which decreases the thermal conductivity thereby increasing the Blech length. However, for short interconnects, pure SWCNT is suggested to perform well. This tradeoff for longer interconnects can be put forward to estimate the performance of bundles of CNT-based interconnects.

## REFERENCES

- [1] International Technology Roadmap for Semiconductors. [Online]. Available: [http://www.itrs.net/Links/2009ITRS/2009Chapters\\_2009Tables/2009\\_Interconnect.pdf](http://www.itrs.net/Links/2009ITRS/2009Chapters_2009Tables/2009_Interconnect.pdf)
- [2] J. Yu, G. Liu, A. V. Sumant, V. Goyal, and A. A. Balandin, "Graphene-on-diamond devices with increased current-carrying capacity: Carbon *sp*<sup>2</sup>-on-*sp*<sup>3</sup> technology," *Nano Lett.*, vol. 12, no. 3, pp. 1603–1608, Mar. 2012.
- [3] E. Pop, D. A. Mann, K. E. Goodson, and H. Dai, "Electrical and thermal transport in metallic single-wall carbon nanotubes on insulating substrates," *J. Appl. Phys.*, vol. 101, no. 1–9, p. 093 710, May 2007.
- [4] A. A. Balandin, "Thermal properties of graphene and nanostructured carbon materials," *Nat. Mater.*, vol. 10, no. 8, pp. 569–581, Aug. 2011.
- [5] C. Yu, L. Shi, Z. Yao, D. Li, and A. Majumdar, "Thermal conductance and thermopower of an individual single-wall carbon nanotube," *Nano Lett.*, vol. 5, no. 9, pp. 1842–1846, Sep. 2005.
- [6] E. Pop, D. Mann, Q. Wang, K. Goodson, and H. Dai, "Thermal conductance of an individual single-wall carbon nanotube above room temperature," *Nano Lett.*, vol. 6, no. 1, pp. 96–100, Jan. 2006.
- [7] S. Chen, Q. Wu, C. Mishra, J. Kang, H. Zhang, K. Cho, W. Cai, A. A. Balandin, and R. S. Ruoff, "Thermal conductivity of isotopically modified graphene," *Nat. Mater.*, vol. 11, pp. 203–207, 2012.
- [8] S. Bhattacharya, R. Amalraj, and S. Mahapatra, "Physics-based thermal conductivity model for metallic single-walled carbon nanotube interconnects," *IEEE Electron. Device Lett.*, vol. 32, no. 2, pp. 203–205, Feb. 2011.
- [9] R. Verma, S. Bhattacharya, and S. Mahapatra, "Analytical solution of Joule-heating equation for metallic single-walled carbon nanotube interconnects," *IEEE Trans. Electron Devices*, vol. 58, no. 11, pp. 3991–3996, Nov. 2011.
- [10] J. J. Clement and J. R. Lloyd, "Numerical investigations of the electromigration boundary value problem," *J. Appl. Phys.*, vol. 71, no. 4, pp. 1729–1731, Feb. 1992.
- [11] M. Shatzkes and J. R. Lloyd, "A model for conductor failure considering diffusion concurrently with electromigration resulting in a current exponent of 2," *J. Appl. Phys.*, vol. 59, no. 11, pp. 3890–3893, Jun. 1986.
- [12] J. R. Black, "Electromigration—A brief survey and some recent results," *IEEE Trans. Electron Devices*, vol. ED-16, no. 4, pp. 338–347, Apr. 1969.
- [13] C. M. Tan and A. Roy, "Electromigration in ULSI interconnects," *Mater. Sci. Eng.—R, Rep.*, vol. 58, no. 1/2, p. 117, Oct. 2007.
- [14] J. J. Clement, "Electromigration modeling for integrated circuit interconnect reliability analysis," *IEEE Trans. Device Mater. Rel.*, vol. 1, no. 1, pp. 33–42, Mar. 2001.
- [15] H. Suhl and P. A. Turner, "Nucleation of voids and their growth during electromigration," *J. Appl. Phys.*, vol. 44, no. 11, pp. 4891–4895, Nov. 1973.
- [16] K. N. Tu, "Recent advances on electromigration in very-large-scale integration of interconnects," *J. Appl. Phys.*, vol. 94, no. 9, pp. 5451–5473, Nov. 2003.
- [17] I. N. Blech and C. Herrings, "Stress generation by electromigration," *Appl. Phys. Lett.*, vol. 29, no. 3, pp. 131–133, Aug. 1976.
- [18] S. Reich, H. Jantoljak, and C. Thomsen, "Shear strain in carbon nanotubes under hydrostatic pressure," *Phys. Rev. B, Condens. Matter Mater. Phys.*, vol. 61, no. 20, pp. R13 389–R13 392, May 2000.
- [19] Z. L. Wang, D. W. Tang, X. H. Zheng, W. G. Zhang, and Y. T. Zhu, "Length-dependent thermal conductivity of single-wall carbon nanotubes: Prediction and measurements," *Nanotechnology*, vol. 18, no. 47, p. 475 714, Nov. 2007.
- [20] J. Hone, B. Batlogg, Z. Benes, A. T. Johnson, and J. E. Fischer, "Quantized phonon spectrum of single-wall carbon nanotubes," *Science*, vol. 289, no. 5485, pp. 1730–1733, Sep. 2000.
- [21] N. Mingo and D. A. Broido, "Length dependence of carbon nanotube thermal conductivity and the problem of long waves," *Nano Lett.*, vol. 5, no. 7, pp. 1221–1225, Jul. 2005.
- [22] D. L. Nika, E. P. Pokatilov, and A. A. Balandin, "Theoretical description of thermal transport in graphene: The issues of phonon cutoff frequencies and polarization branches," *Phys. Stat. Sol. (B)*, vol. 248, no. 11, pp. 2609–2614, Nov. 2011.
- [23] R. Kirchheim and U. Kaeber, "Atomistic and computer modeling of metalization failure of integrated circuits by electromigration," *J. Appl. Phys.*, vol. 70, no. 1, pp. 172–181, Jul. 1991.
- [24] N. Srivastava, H. Li, F. Kreupl, and K. Banerjee, "On the applicability of single-walled carbon nanotubes as VLSI interconnects," *IEEE Trans. Nanotechnol.*, vol. 8, no. 4, pp. 542–559, Jul. 2009.
- [25] A. Naeemi and J. D. Meindl, "Design and performance modeling for single-walled carbon nanotubes as local, semiglobal, and global interconnects in gigascale integrated systems," *IEEE Trans. Electron Devices*, vol. 54, no. 1, pp. 26–37, Jan. 2007.
- [26] A. Nieuwoudt and Y. Massoud, "On the optimal design, performance, and reliability of future carbon nanotube-based interconnect solutions," *IEEE Trans. Electron Devices*, vol. 55, no. 8, pp. 2097–2101, Aug. 2008.
- [27] A. Khitun, A. Balandin, and K. L. Wang, "Modification of the lattice thermal conductivity in silicon quantum wires due to spatial confinement of acoustic phonons," *Superlattices Microstruct.*, vol. 26, no. 3, pp. 181–193, Sep. 1999.
- [28] X. Lu, K. D. Ausman, R. D. Piner, and R. S. Ruoff, "Scanning electron microscopy study of carbon nanotubes heated at high temperatures in air," *J. Appl. Phys.*, vol. 86, no. 1, pp. 186–199, Jul. 1999.
- [29] N. Mingo and D. A. Broido, "Carbon nanotube ballistic thermal conductance and its limits," *Phys. Rev. Lett.*, vol. 95, no. 9, p. 096 105, Aug. 2005.



**Rekha Verma** (S'12) received the M.Tech. degree from Banasthali University, Banasthali, India, in 2009. She is currently working toward the Ph.D. degree in the Department of Electronic Systems Engineering, Indian Institute of Science, Bangalore, India.



**Sitangshu Bhattacharya** received the Ph.D. degree from Jadavpur University, Kolkata, India, in 2009. He is currently a Postdoctoral Fellow with the Department of Electronic Systems Engineering, Indian Institute of Science, Bangalore, India.



**Santanu Mahapatra** (M'08–SM'10) received the Ph.D. degree from the École Polytechnique Fédérale de Lausanne, Lausanne, Switzerland, in 2005. He is currently an Associate Professor with the Indian Institute of Science, Bangalore, India.